1965

The analysis of bolted butt joints, Proc. ASCE, Vol. 91, ST5, 1965, Publication No. 274

J. W. Fisher

J. L. Rumpf

LEHIGH UNIVERSITY INSTITUTE OF RESEARCH

Long Bolted Connections

THE ANALYSIS OF BOLTED BUTT JOINTS

by

John W. Fisher
John L. Rumpf

Fritz Engineering Laboratory Report No. 288.17

SYNOPSIS

In this report a theoretical solution is developed for the unequal distribution of load among the bolts in double-lap tension splices which have non-linear behavior. To accomplish this solution, mathematical models are developed which establish the relationship between deformation and load throughout the elastic and inelastic regions for the component parts of the connections.

The theoretical solution is compared with results of tests of full-size connection, eight made with 7/8-in. A325 bolts and A7 steel plate and eleven with 7/8-in. A325 bolts and A440 steel plate. The maximum deviation between the theoretical solution and the test results was 4%.

INTRODUCTION

Large riveted joints have been used for many years in steel bridges. Early work with riveted joints showed that rivets have an ultimate shear strength which is about 75% of their tensile strength[1]. Since the tensile strength of low carbon steel rivets (58 to 62 ksi) is about equal to the ultimate strength of low carbon steel plates (ASTM-A7) it is reasonable that the allowable shear stress for the rivets should be approximately 75% of the allowable tensile stress for the plates. As a result, the "tension-shear ratio" and "balanced design" concepts were developed and accepted. The "tension-shear ratio" is the ratio of the tensile stress on the net section of the plate to the average shear stress on the nominal area of the fasteners. The concept of balanced design implies that the ultimate shear strength of a group of fasteners will equal the tensile capacity of the net section of the main material.

The introduction of the high-strength bolt (ASTM-A325) as a replacement for the steel rivet was first made on the basis of substituting one bolt for one rivet[2]. Since the shear strength of the bolt was greater than that of the rivet, the A325 bolted joint was not "in balance." Tests were conducted on compact bolted joints to determine the proper ratio of the shear area to the net tension area for balanced design[3]. These studies show that the proper tension-shear ratio is 1 to 1.10 for A325 bolts in A7 steel joints. The

corresponding ratio for A141 steel rivets in A7 steel is 1 to 0.75.

The balanced design concept was also used to determine the relative proportions of shear and net areas when A325 bolts connect higher strength steel plates (ASTM-A440)[4]. In these tests balanced design was achieved for compact joints with a tension-shear ratio of 1 to 1.

These investigations show that when A325 bolts are installed in A7 steel, an allowable design stress of 22 ksi gives a reasonable factor of safety against failure. When the same bolt is installed in A440 steel the balanced design concept leads to a different factor of safety against failure and yields an allowable shear stress of 27.5 ksi. This poses an interesting question in design philosophy: Is it rational to use different allowable shear stresses for the same fastener in different materials? This query has been reviewed and discussed in Ref. 5. This examination shows that:

(1) the concept of balanced design leads to inconsistent allowable bolt stresses for the same bolt in different plate materials,

(2) the A325 bolts' shear behavior is the same in all compact joints regardless of the type of connected material, and

(3) the balanced design concept has no meaning in long joints in any case because the bolts fail before the plate material attains full strength.

Thus, a need existed for a theoretical approach to ascertain the relative significance of variations in the relative proportions of bolt shear area and plate net tensile area; and the effect of fastener pitch, bolt diameter, and joint length on bolt behavior.

PREVIOUS THEORETICAL STUDIES

An extensive review of previous theoretical studies of mechanically fastened joints is given in Refs. 6 and 7. Most of the past theoretical studies of mechanically fastened joints considered the relationship between load and deformation only in the elastic or linear range. The early study by Arnovlevic in 1909 was followed by the work of Batho[9], Bleich[10], Hrennikoff[7], and Vogt[11]. These studies show that the end fasteners carry the greatest percentage of load and that not much is gained by adding additional fasteners because in the elastic range the interior fasteners are practically useless as load resisting elements.

Vogt[11] was among the first to propose studies in the inelastic or non-linear region. His analysis was restricted since it considered the non-linear deformations as occurring only in the fasteners and holes. The combined load-deformation characteristics of the fastener and hole were assumed to be represented by two linear relationships. This work was followed by an extensive study of aluminum riveted joints by Francis[12] who considered the behavior of double shear joints in the elastic range and beyond. Equilibrium

and compatibility conditions were formulated and the distribution of load to individual rivets was determined. Also described was a semi-graphical construction which facilitated the solution for the load partition in the inelastic regions.

Rumpf[13] adapted the methods described by Francis[12] to bolted bearing-type joints of A7 steel and A325 bolts. The solution was found to be applicable to the region between the slip load and the ultimate load. Excellent correlation between the theoretical values and the experimental data was obtained.

The semi-graphical construction used by Francis[12] and Rumpf[13] is convenient to use only for short joints. This iterative method usually requires several trials before the solution is obtained and with longer joints the analysis is extremely tedious and time consuming. Also, a plate calibration test is necessary for each geometrical condition of interest.

Fisher[14] developed mathematical models which establish the relationship between deformation and load for the component parts of the connections throughout the elastic and inelastic regions. A digital computer program was developed for bolted plate problems in order to make the solution more practical. The solution was used to study the effect of joint length, pitch, variation in fastener diameter, and variations in the relative proportions of the bolt shear area and the net tensile area.

This paper is based on the theoretical developments reported in Refs. 13 and 14.

SUMMARY OF EXPERIMENTAL STUDIES

Small-scale riveted and bolted joints have been subjected to extensive experimentation, while relatively few large joints have been tested. The tests of riveted joints have been summarized by DeJonge[6]. The summaries given hereafter are for tests on large butt-splice specimens connected by rivets or bolts.

In 1940, Davis, Woodruff, and Davis[1] reported on an extensive series of tests of large riveted joints conducted in connection with the design and construction of the San Francisco-Oakland Bay Bridge. They reported premature fastener failures in joints of considerable length connected with 7/8-in. rivets and pointed out that excessive deformation caused the end fasteners to fail.

In 1957, a demonstration test of a compact A242 high-strength steel specimen connected by nine A325 and nine A354 BD bolts was performed at Northwestern University[15]. The joint was proportioned so that plate failure occurred.

The University of Washington[16] reported a bolt failure in a connection having thirteen rows of A325 bolts. Several other compact specimens failed with a shearing of the bolts.

Static tension tests of large compact butt joints conducted at Lehigh University[3] show that the end fasteners have a tendency to fail before all bolts develop their maximum strength. However, these tests were conducted on specimens no longer than 14 inches between end bolts. As a result, the average shear stress at first bolt failure was not greatly affected by the joint length.

Because of the tendency toward premature failure of the end fasteners, additional tests were conducted at Lehigh University on long bolted connections[17]. In these connections the net tension area was made 10% greater than the bolt shear area because the tests reported in Ref. 3 showed this to be the balanced design proportion. All joints were fabricated of A7 steel and most were connected by 7/8-in. A325 bolts. In longer joints the end fasteners sheared before all bolts could develop their full shearing strength. In the short connections the average shear strength was about 90% of the strength of a single bolt, but bolts in the longest connection developed only 60% of the strength of a single bolt. Limited tests of bolted lap joints provided information on the behavior of bolts in single shear, while several tests of riveted connections provided a basis for comparison of bolted and riveted connections.

More recently, tests of structural joints of A440 steel connected by A325 high-strength bolts were conducted at Lehigh University[4]. The joints had from 4 to 16 fasteners in line. These tests showed that the shear strength of bolts in compact A440 joints does not differ significantly from the compact A7 steel joints. For the longer joints, the decrease in bolt shear strength was not nearly as great as that of similar A7 steel joints.

The tests reported in Refs. 3, 4, and 17 will be used to check the validity of the theory.

BEHAVIOR OF DOUBLE-LAP BUTT JOINTS

The behavior of riveted or bolted double-lap butt joints is basically the same, so the following discussion applies to both types of fasteners. Observations of the tests reported in Refs. 3, 4 and 17 are the bases of the following descriptions of joint behavior. Two distinct phases are involved: the first occurs before slip when the principal load transfer mechanism operates through friction between the faying surfaces, and the second occurs after slip when the principal load transfer mechanism is one of bearing and shear. Figure 1 shows the behavior of a typical joint under load.

Both riveted and bolted joints generally exhibit both of these load transfer mechanisms. In riveted joints one can seldom predict when slip will take place because the clamping force in the rivets cannot be predicted reliably and in fact may not exist.

The behavior of a bolted joint during its loading history can be subdivided into phases which include: (a) complete rigidity, that is no movement of the connected parts, (b) partial slip, (c) complete slip, (d) partial bearing, (e) complete bearing, and (f) bolt shearing and failure. A summary of these phases follows. A more detailed description is given in Ref. 13. Phases (a), (b), and (c) involve load transfer by friction and phases (d), (e), and (f) involve load transfer by bearing and shear.

1. Load Transfer by Friction

A recent theoretical and experimental study of the frictional load transfer in bolted joints[18] shows that higher frictional stresses

exist at the joint ends because of the strain compatibility condition. For example, at one end of the joint the main plate is carrying a high load while the adjacent lap plates have relatively low loads. Eventually there is a relative displacement of certain contact points on the faying surfaces near the ends of the joint, a condition known as partial slip. When the load is increased, the slip zones proceed inward from the ends of the joint. The slip zones finally cover the entire faying surface with a resulting maximum static frictional resistance. Any increase in load cannot be balanced, and large relative displacements (major slip) cause the fasteners to come into bearing with the sides of the holes. Generally the plate accelerations are so large that the slip stops only when one plate encounters bolts bearing against the other plate.

2. Load Transfer by Bearing and Shear

After slip has occurred, several of the fasteners are in bearing, being in contact with the main plate on one side of the fasteners and with the lap plates on the other. Unless some of the holes are misaligned, the end fasteners come into bearing first because the greatest differential plate elongations have occurred there. Generally, both the fastener and the plate are elastic at this point.

Before it comes into bearing the only force acting on the fastener is its initial tension. As the fastener comes into contact it tends to shear, bend, and deform by bearing with a resulting relaxation of its initial tension. In addition, the plate tends to deform locally at its points of contact with the fastener. As load

is applied the end fasteners and holes deform until other fasteners come into bearing. When the joint has more than two fasteners in a line, the plate deformations influence the load partition among the fasteners.

Once all fasteners are in bearing, additional load causes further plate deformations which impose compatible deformations in the fasteners. The deformations result in additional bolt forces. Elastic and inelastic analysis have shown that the bolt deformations are dependent on the difference between the elongations of the lap plate and the main plate between any two rows of fasteners. If the plate material were perfectly rigid, each fastener would deform the same amount and presumably would carry an equal share of the load.

Regardless of whether the plate or the fasteners first deform permanently, the accumulated differential strains between the main plate and the lap plate eventually exceed the deformation capacity of the fasteners and failure begins. If the joint is reasonably compact all the fasteners will have approached their maximum load carrying capacity. As one or more end bolts fracture, the load cannot be carried successfully by the remaining bolts; and all fasteners shear almost simultaneously. For longer joints the accumulated differential deformations cause the end fasteners to fail but their load is successfully distributed to the other fasteners. Continued loading results in a sequential type of failure called "unbuttoning" which progresses inward from the ends of the joint[1][4][17].

If the plate strength at the net section is considerably less than the shear strength of the fasteners, failure will occur with the tearing of the plate in compact and intermediate length joints. When the plate strength at the net section is considerably larger than the shear strength of the fasteners, all fasteners are loaded to nearly their full capacity.

Even after slip occurs and the fasteners are in bearing, some load is transferred by friction. However, as the fasteners deform permanently at their shear planes, the initial clamping force relaxes and the frictional force is reduced. Observations and measurements made during testing of large bolted connections showed that the bolts lost preload after major slip occurred and the fasteners were in bearing[19]. With the exception of those in the end rows at the lap plate end, bolts lost internal tension as load increased. Internal tension almost disappeared near ultimate load.

DEVELOPMENT OF THEORETICAL SOLUTION

SCOPE

This investigation is concerned primarily with developing a solution for joints in which the fasteners are in a state of bearing and double shear. The theoretical work of Francis[12] is used as a foundation.

The theoretical solution of the load partition is based on the major assumptions that: (1) the fasteners transmit all the applied load by shear and bearing once major slip has occurred; and (2) the frictional forces may be neglected in the region for which the solution is intended, the region between major slip and ultimate load. The validity of these assumptions will be discussed later.

EQUILIBRIUM AND COMPATIBILITY RELATIONSHIPS

The type of connection studied is a double shear, symmetrical butt joint as shown in Fig. 2. The inner plate, hereafter called the main plate, is the principal member. The outer plates are called lap plates. The longitudinal line of holes parallel to the axial load is called a line and the longitudinal space between each hole is called a pitch. The transverse series of holes is called a row and the transverse space between holes is called the gage.

The lap plates are assumed to be of the same thickness and material. However, the main plate may be of different material and may have any thickness. The hole pattern is assumed to be completely

filled and the bolts are assumed to be of the same size and material. For purposes of analysis, the joint is divided into gage strips as shown in Fig. 3. It is assumed that all gage strips are identical in behavior.

The fasteners are assumed to transmit all applied load by bearing and shear once major slip has occurred. Such an assumption can be satisfied only if the holes are perfectly aligned and the effect of friction is neglected. The solution is valid both for joints erected in bearing and for joints which slip into bearing, for it is assumed that the joint behavior between slip and ultimate load is independent of the time when slip occurs.

The analysis consists beasically of considering the joint as a statically indeterminate structure. Very similar analyses were used in Refs. 7, 8, 10 and 11 for elastic conditions alone. The analysis given here is, in addition, equally applicable to the inelastic case because the non-linear behavior of the components is considered.

The solution of the problem follows the method of ordinary mechanics. Two basic conditions must be formulated. One satisfies the condition of equilibrium (statics) and the other insures that continuity (or compatibility) will be maintained throughout the elastic and inelastic ranges. These conditions coupled with the initial value considerations such as the ultimate strength of the plate and the ultimate strength of the critical fastener yield the solution to the problem.

The equilibrium conditions can be visualized with the aid of Fig. 4. The load per gage strip in the main plate between bolts i and i+1 is equal to the total load on this strip (P_G) minus the sum of the loads on all bolts (ΣR_i) preceding the part of the joint considered. Hence between i and i+1

$$P_{i,\ i+1} = P_G - \sum_{i=1}^{i} R_i \qquad (1)$$

The load per gage strip in the lap plates between bolts i and i+1 is equal to the sum of the loads transmitted to the lap plate by all the bolts preceding the part of the joint considered. Hence,

$$Q_{i,\ i+1} = \sum_{i=1}^{i} R_i \qquad (2)$$

The compatibility conditions described hereafter consider the joint in the slipped position so that the fasteners are in bearing with the plate.

The compatibility equations that correspond to the equilibrium equation described by Eqs. 1 and 2 will be formulated by considering Fig. 5. As load is applied to the slipped joint the deformations are considered within the joint between points i and i+1 (Fig. 5). Due to the applied load, the main plate will have elongated so that the distance between the main plate holes is $p + e_{i,\ i+1}$. The lap plate will have elongated and the distance between the lap plate holes is $P + e'_{i,\ i+1}$. The distance p is the initial fastener pitch as shown

in Fig. 2. The elongations $e'_{i,\,i+1}$ and e'_{i} are for the main plate and lap plate respectively. They are the elongations between points i and i+1. Hereafter, a primed symbol will signify the lap plates.

In an actual test joint, the reference points for the measurement of pitch elongations are the edges of the plate at the centerline of each hole. After slip the apparent offsets of these reference points do not properly indicate the deformations of the bolts. Consider the deformations of the plates and bolt at bolt i as shown in Fig. 6. When the bolt bears against the side of the main plate it compresses the steel an amount δ_{pi}. Assuming that the bearing deformation of the bolt itself is negligible, the bolt moves to the right an amount δ_{pi}. Meanwhile, the main plate is stretching under the tensile load and the circular holes become oval. This allows the bolt to move to the right an amount η_i, the elongation of the radius of the hole. Hence, in the slipped position at bolt i, the distance between the centerline of the hole in the main plate and the centerline of the bolt is $\delta_{pi} + \eta_i$.

A similar expression can be devised for the lap plates. The hole elongation η'_i is not equal to η_i because the tensile forces are not the same in the respective plates. The bearing deformation of the lap plate need not be equal to that of the main plate. The total relative movement at i is: $\delta_b + \delta_{pi} + \delta'_{pi} + \eta_i + \eta'_i$ where δ_b is relative shear and bending displacement of the bolt. The deformation $\delta_b + \delta_{pi} + \delta'_{pi}$ will be called Δ_i. Therefore, the relative movement at i is $\Delta_i + \eta_i + \eta'_i$. At i+1 the relative movement is $\Delta_{i+1} + \eta_{i+1} +$

η'_{i+1}.

It can be shown by considering Fig. 5 that the relative movement of fastener i to the left by the amount η'_i has been accounted for by the plate elongation $e'_{i,\ i+1}$. Similarly the movement η'_{i+1} has been accounted for by the plate elongation $e'_{i,\ i+1}$. The gap between the bolt and main plate hole at i is c+2 η_i where c is the original hole clearance. At bolt i+1 the gap between the bolt and the lap plate hole is c+2 η'_{i+1}. Neither of these relative movements affect the formulation of the compatibility condition.

An equation can be formulated by considering the total length of the lap and main plates between points i and i+1 and the deformations of the fasteners and holes. From Fig. 5 it can be seen that

$$\Delta_i + p + d + e'_{i,\ i+1} = \Delta_{i+1} + p + d + e_{i,\ i+1} \qquad (3)$$

or

$$\Delta_i + e'_{i,\ i+1} = \Delta_{i+1} + e_{i,\ i+1} \qquad (4)$$

where Δ_i and Δ_{i+1} are the deformations of the i and i+1 fasteners. The quantities Δ include the effects of shear, bending, and bearing on the fastener and the localized effect of bearing on the plates. Further discussion of these parameters is given later when the load-deformation relationship of single fasteners is developed. It is assumed that the deformations of the fastener Δ_i are the same whether considered at the hole edge (fastener surface) or the centerline of the fastener.

If the plate elongations are expressed as functions of load

in the segments of the joint between fasteners, and the fastener deformations as functions of the fastener loads, Eq. 4 can be written as:

$$f(R_i) + \Psi(Q_{i,\ i+1}) = f(R_{i+1}) + \Phi(P_{i,\ i+1}) \tag{5}$$

where $f(R_i)$, $f(R_{i+1})$ are bolt deformations, $\Phi(P_{i\ i+1})$ is the main plate elongation, and $\Psi(Q_{i\ i+1})$ is the lap plate elongation. Finally, Eqs. 1 and 2 can be substituted into Eq. 5 and the compatibility equations are expressed as functions of the unknown bolt forces. Hence,

$$f(R_i) + \Psi\left(\sum_{i=1}^{i} R_i\right) = f(R_{i+1}) + \Phi\left(P_G - \sum_{i=1}^{i} R_i\right) \tag{6}$$

In the elastic or inelastic range of load for a joint having n fasteners in line, Eq. 6 can be written for each section of the joint, giving n-1 simultaneous equations. These, with the equation of equilibrium

$$P_G - \sum_{i=1}^{n} R_i = 0 \tag{7}$$

may be solved to give the loads acting on the fasteners if the relationship between load and elongation for the various components is known. With this information the total load acting on the joint may be found for a given deformation, and finally the load at failure may be determined.

The two basic load-deformation relationships required, then, are that of the plate with holes and that of the fastener. These become the standard "coupons" which are the basis for predicting joint behavior. These "coupons" and their analytical models are described

in the following sections.

TENSILE STRESS-STRAIN RELATIONSHIPS FOR PLATE MATERIALS

A plate in tension having one or more hole is an integral part of a mechanically fastened joint. As was indicated earlier, the true nature of the load deformation relationships for the bolt and plates must be known if Eqs. 6 and 7 are to be solved. These relationships must first be established by experiment.

The standard plate calibration coupon which yields the load-deformation relationship for the connected plate is shown in Fig. 7. The "plate calibration coupon" should be cut from the same material as the actual test connections. Its geometrical properties should also be similar; the thickness, gage, pitch, and hole diameter must be the same as used in the test or prototype connections.

Equation 4 and Fig. 5 show that the elongation needed is the elongation of a pitch from the edge of one hole to the corresponding edge of the next hole. Since the same force acts at every cross section of the calibration plate, the elongation from center to center of the holes corresponds to the needed elongation. When the "calibration coupon" is loaded, the stress-strain relationship shown in Fig. 8 is observed.

Several special tests conducted and reported by Rumpf show that the single gage calibration specimen is representative of the behavior of multiple gage calibration strips[13]. Also, it is shown

that the clamping action of the bolts has little or no effect on the load-deformation characteristics of the plate calibration specimen. The semi-graphical solution used by Francis[12] and Rumpf[13] was the actual stress-strain relationship for the "plate calibration coupon."

Fisher developed an analytical model which describes the stress-strain behavior of the plate calibration coupon throughout the elastic and inelastic ranges[14]. The mathematical model is applicable to both A7 and A440 steels and accounts for changes in geometry such as plate width, plate thickness, and hole spacing. As a result, it is possible to interpolate and extrapolate to various specimen geometries. A detailed description of the behavior of plates with holes and the development of the analytical model is given in Ref. 14.

It was found that in the elastic range, the effect of holes on pitch elongations can usually be ignored. Neglecting the non-uniformity of strain because of the holes, the average strain between the holes was approximated as

$$\epsilon = e/p = P/A_g E \tag{8}$$

where p = pitch or distance between the centerline of holes,

A_g = gross cross-sectional area,

P = load, and

e = total deformation between the holes.

This expression is applicable until yielding commences in the net section area, at which time the stress is less than the yield point on the gross area.

As yielding begins in the net section of the plate, the linear relationship between stress and strain is no longer valid. The general relationship for stress-strain applicable to both A7 and A440 steel and various specimen geometries is

$$\sigma = \sigma_y + (\sigma_u - \sigma_y) \left[1 - \underline{e}^{-(\sigma_u - \sigma_y)(g/g-d)(e/p)} \right]^{3/2} \qquad (9)$$

where σ_y = yield stress,

σ_u = ultimate strength,

g = gage,

d = hole diameter,

e/p = plastic strain, and

$\underline{e}$ = base of natural logarithm

This equation is applicable for values $\sigma_y < \sigma < \sigma_{ult}$

For stresses lower than the yield point, Eq. 8 is applicable. Equations 8 and 9 are compared with the test data for A7 and A440 steel in Figs. 9 and 10. The total load acting on the plate calibration specimen is plotted as a function of the deformation e. The agreement between the theoretical and experimental results is good for both A7 and A440 steel plates with fastener holes and with wide variations in specimen geometry.

SHEAR DEFORMATION RELATIONSHIP FOR FASTENERS

If a single fastener joint is loaded as shown in Fig. 11, the relative movement of points a and b is influenced by the shear,

bending, and bearing of the fastener. Figure 12 shows a deformed bolt illustrating this behavior. The connected members will also deform and the relative movement of a and b, if measured at the edges of the plate, will be greater as a result of the compression of the members behind the fastener. For the elastic case, Coker[20] has shown that the longitudinal compressive stress in the plate dies away at a distance of about twice the hole diameter from the edge of the hole. Hence, the bearing deformations in the plate are localized. In the side view of the joint in Fig. 11 they are indicated by the dark edges. In measuring the relative movement of a and b, the deformation of the fastener and plate are combined. There is no reason to separate them.

Two types of control or "coupon" tests can be conducted to determine the load-deformation relationship. In one type the bolts are subjected to double shear by plates loaded in tension as indicated in Fig. 11. In the other control test the bolts are subjected to double shear by applying a compressive load to the plates (Fig. 12). As long as the shear jig plate is reasonably stiff and only local yielding due to bearing occurs, any plate deformations other than those due to bearing are negligible.

The load-deformation relationships for the two types of control tests for a typical bolt lot are shown in Fig. 13. These calibration tests show that single bolts tested in plates loaded in tension have approximately 5 to 10% less shear strength than bolts loaded by plates in compression.

Rumpf[13] and Francis[12] both used the measured load-deformation relationships of the single fastener for their semi-graphical solutions. In this manner the non-linear behavior of the fasteners is accounted for.

To facilitate the solution of the compatibility equations, Fisher[14] developed an analytical expression for the elastic-inelastic load-deformation relationship of a single fastener. The following expression was used for the load-deformation relationship.

$$R = R_{ult} \left[1 - \underline{e}^{-\mu\Delta} \right]^{\lambda} \qquad (10)$$

where R_{ult} = ultimate shear strength,

Δ = total deformation of bolt and bearing deformation of the connected material,

μ, λ = regression coefficients, and

$\underline{e}$ = base of natural logarithm.

The average values of R_{ult}, μ and λ are tabulated in Table 1 for the five lots of bolts used in the test joints reported in Refs. 3, 4 and 17.

The total deformation capacity Δ_{ult} for a given bolt and connected material is a function of the shear, bending, and bearing of the bolt and the bearing deformation of the plates. As might be expected, this will vary with the type of calibration test, the type of connected steel, and the thickness of the gripped material. Values of Δ_{ult} are also tabulated in Table 1.

Equation 10 has been compared with test data of typical bolt lots in Figs. 14 and 15. The theoretical line is in good agreement with

the test data.

Reference 14 provides additional discussion of the behavior of single bolts in shear, proposals for computing the elastic shear-deformation relationship, and the development of the analytical model described by Eq. 10.

GENERAL SOLUTION OF THE EQUILIBRIUM AND COMPATIBILITY EQUATIONS

1. Assumptions in Theory

The solution of the general equilibrium and compatibility equations is accomplished by employing the load-deformation relationships developed in Ref. 14, relationships valid for both the elastic and inelastic ranges.

The following assumptions are made to facilitate the solution:

1. The fasteners transmit all the applied load once major slip has occurred. Any frictional forces in the region between slip and the ultimate load are neglected.
2. The analytical expressions are applicable to the component elements of the connection. (The load-deformation or stress-strain relationships for each pitch are the same.)
3. All fasteners are the same diameter.

2. General Load-Elongation Relationships

The functions $f(R_i)$, $f(R_{i+1})$, $\Psi(Q_{i,\ i+1})$ and $\Phi(P_{i,\ i+1})$

in Eq. 5 can be obtained from the analytical expressions described by Eqs. 8, 9 and 10. These functions are as follows:

$$\Delta_i = f(R_i) \tag{11}$$

From Eq. 10 this expression can be determined as

$$\Delta_i = \frac{-1}{\mu}\left(\ln \quad 1 - \left[\frac{R_i}{R_{ult}}\right]^{1/\lambda}\right) \tag{12}$$

where $0 < R_i < R_{ult}$.

Similarly,

$$\Delta_{i+1} = \frac{-1}{\mu}\left(\ln \quad 1 - \left[\frac{R_{i+1}}{R_{ult}}\right]^{1/\lambda}\right) \tag{13}$$

The deformations in the main and lap plates can be determined from Eqs. 8 and 9. For the main plate the following expressions are obtained:

$$e_{i,\ i+1} = \frac{\left[P_G - \Sigma R_i\right] p}{A_g E} \tag{14}$$

when $0 < P_G - \Sigma R_i < \sigma_y A_n$ and

$$e_{i,\ i+1} = \frac{\sigma_y A_n p}{A_g E} + p\left[\frac{-1}{(\sigma_u - \sigma_y)(g/g\text{-}d)} \ln \left(1 - \left[\frac{P_G - \Sigma R_i - \sigma_y A_n}{(\sigma_u - \sigma_y)\ A_n}\right]^{2/3}\right)\right] \tag{15}$$

when $\sigma_y A_n < P_G - \Sigma R_i < \sigma_y A_n$

For the lap plates the following elongations are obtained:

$$e'_{i,\ i+1} = \frac{p \Sigma R_i}{A'_g E'} \tag{16}$$

when $0 < \Sigma R_i < \sigma'_y A'_n$. In the inelastic regions, the elongations become:

$$e'_{i,\,i+1} = \frac{\sigma'_y A'_n p}{A'_g E'} + p\left[\frac{-1}{(\sigma'_u - \sigma'_y)(g/g\text{-}d)} \ln\left(1 - \left[\frac{\Sigma R_i - \sigma'_y A'_n}{(\sigma'_u - \sigma'_y)A'_n}\right]^{2/3}\right)\right] \quad (17)$$

where $\sigma'_y A'_n < P_G - \Sigma R_i < \sigma'_u A'_n$

Equations 12 to 17 substituted into Eq. 4 result in a new form of Eq. 6. These expressions allow examination of a large number of variables. For instance, the strength and/or thickness of the plates can be varied. Also, the solution is applicable to hybrid joints, joints of two different steels and different types and sizes of fasteners can be accommodated.

3. Solution of Compatibility and Equilibrium Equations

The solution of the compatibility and equilibrium equations can now be made. From the compatibility equation (Eq. 6) for $i = 1$ it is clear that three of the four terms are functions of R_1 alone. Hence, if R_1 is assumed or known, R_2 can be solved for a given joint load. Once R_2 is known the succeeding value R_3 can be determined. In general, then, each succeeding value of R_{i+1} can be determined once the value of R_i is known. All values of R_i are dependent on the originally assumed values of R_1 and P_G. However, a solution is valid only if the equilibrium equation (Eq. 7) is satisfied. If it is not, then a new value of R_1 or P_G must be chosen and the interaction repeated.

The following procedure is employed to obtain the solution to Eqs. 6 and 7. An initial value of R_1 and the corresponding deformation Δ_1 are selected as is shown graphically in Fig. 16. Next an estimate is made of the gage load P_G which would correspond to the assumed bolt force R_1. With these known initial values, it is possible to compute the remaining bolt forces R_i. Figure 16 shows the relative locations of these bolt forces on the load-deformation diagram. The equilibrium equation (Eq. 7) is checked and if it is not satisfied another guess is made for the gage load P_G and the process is repeated. This process continues until Eq. 7 is satisfied.

The solution of the equilibrium and compatibility equations just described would be lengthy and laborious, especially for long joints with many fasteners, were it not for the digital computer. Fortunately, the digital computer is ideally suited to the solution of problems of this type when iterative procedures are necessary. The digital computer program described in Ref. 14 was developed to solve these equations. The program is summarized in Fig. 17 in a flow-chart.

The bolt forces are computed from the assumed initial values of the bolt force R_1 and the trial values of the load P_G. The equilibrium condition is tested and if it is satisfied within 0.1%, the solution is acceptable.

Additional details concerning the development, use, and limitations of the program can be found in Ref. 14.

COMPARISON OF THEORY WITH TESTS

The test results reported in Refs. 3, 4 and 17 afford an opportunity to test the ability of the theory to predict the ultimate strength of A7 and A440 steel joints.

ANALYSIS OF TEST JOINTS AT ULTIMATE LOAD

For the analyses reported herein, the actual bolt and plate properties were substituted into Eqs. 12 to 17. The mechanical properties had been determined from tests of bolts from the same lot and steel plate from the same heat that were used in the test joints. Dimensions measured during the actual test were used.

It was thought desirable to check the ultimate strengths that would be obtained from the two different shear-deformation relationships. The data from one shear-deformation relationship was obtained from tests in which the plate material was loaded in tension and the high-strength bolts subjected to double shear as shown in Fig. 11. In the other shear test the bolts were subjected to double shear by applying a compression load to the plates as shown in Fig. 12.

Observations made during the joint tests reported in Refs. 4 and 17 indicated that prying action existed near the ends of the lap plates where a clear separation of the plates was observed near the ultimate loads.

In addition to the varying behavior of the bolts noted during the calibration tests and joint tests, an inspection of Figs. 14 and 15 shows that the bolt begins to unload very rapidly after reaching its ultimate strength. Additional deformation sometimes occurs before complete rupture. Because of this, in some joints further redistribution may take place before an unbuttoning failure occurs.

Because of these observations, several different analyses were made. They are compared with the experimental results in Table 2 for the A7 steel joints and Table 3 for the A440 steel joints. The following methods or initial values and conditions, were used.

Method 1 All bolts are assumed to behave the same as a single bolt loaded in a tension jig. The maximum load and deformation in the end fasteners of the joint correspond to the ultimate load and deformation of a single fastener in a tension jig.

Method 2 All bolts are assumed to behave the same as a single bolt loaded in a tension jig. The failure load and deformation of the end fasteners of the joint correspond to the rupture load and deformation of a single fastener in a tension jig.

Method 3 All bolts are assumed to behave the same as a single bolt loaded in a compression jig. The maximum load and deformation of the end fasteners of the joint correspond to the ultimate load and deformation of a single fastener in a compression jig.

The predicted ultimate strength in kips for each of the three

analyses is given in Tables 2 and 3, along with the experimental results. Also given is the ratio of the computed ultimate strength to the observed ultimate strength.

The greatest difference between the theoretical and experimental results for A440 steel joints was approximately 4% for Method 1 as can be seen in Fig. 18. Here, the average bolt shear strength is plotted as a function of joint length. The theoretical solutions were based on the analysis designated as Method 1 and used the measured bolt and plate properties. Two different lots of bolts were used in the test series to accommodate the change in grip. Together with the change in geometry, this accounts for the discontinuity at a joint length of approximately 37 inches.

The objective of Method 2 was to see whether the additional deformation between the ultimate load and rupture load of a single bolt would allow further redistribution in a joint. In the longer joints, the additional deformation permitted further redistribution. However, the increase in load was only 1.0%. For practical purposes, Methods 1 and 2 are not significantly different.

Method 3 (compression) yielded ultimate strengths which were somewhat higher than the observed failure load for joints with up to ten fasteners in a line. For A7 steel joints this difference (2%) was only slightly higher. For the A440 steel joints the differences ranged from 4 to 11%. For the longer joints this method gave the best agreement. A comparison between the theory and experimental results is

made in Fig. 19 for Methods 1 and 3 applied to A440 steel joints. The average bolt shear strength is plotted as a function of joint length. Both methods used the measured bolt and plate properties. It is readily apparent that Method 3 predicted too great a strength for the shorter joints. For the longer joints Method 3 agreed more closely with the experimental results. However, the differences between Methods 1 and 3 are small for the longer joints.

PARTITION OF LOAD

It is of interest to examine the load partition in typical A7 and A440 steel joints. The A7 steel joints described in Refs. 3 and 17 had net tensile areas that were usually 10% greater than the bolt shear area ("balanced design"). The A440 steel joints described in Ref. 4 had bolt shear areas equal to net tensile areas. These experimental studies had shown that these ratios would produce a balanced design for compact joints. An examination of Tables 2 and 3 demonstrates that the A440 steel joints connected with A325 bolts sustained greater loads at failure than A7 steel joints connected with the same number of A325 bolts. (Compare D101 with E010 and D16 with E161.)

The reasons for the better performance of the A325 bolt when used with higher strength steels and for the decrease in joint strength with increased length are best illustrated in Figs. 20 and 21. Here, the computed bolt shear stress in each row at two different stages is shown for joints of equal length and with the same number of A325

fasteners. The comparisons are made for joints having four and sixteen fasteners in a line. The upper set in each figure is for A440 steel while the lower set is for A7 steel.

The two different stages of joint behavior described are: (1) when yielding first occurs in the gross section of the plate material, and (2) when the ultimate strength is reached and one or more bolts have failed by shearing. Each of these stages occurs after slip has taken place and the fasteners are in bearing. Also shown is the "shear proportional limit" of the bolt.

Figure 20 shows the bolt forces in a short joint and clearly indicates that nearly complete redistribution of bolt forces has taken place in both the A7 and A440 steel joints because all fasteners are carrying an approximately equal share of the load at ultimate.

In Fig. 21 it can be seen that the fasteners near the center of the A7 steel joints are carrying less than half the force carried by the end fasteners at ultimate. The higher yield strength of the A440 steel has allowed a better redistribution to occur because inelastic deformations occur in bolts while the plate material is still elastic and relatively rigid. With increasing joint length, the higher-yield-strength steel effected a better redistribution of the bolt forces.

Figure 21 shows that the inelastic deformations occurred nearly simultaneously in the plate and end fasteners in the lower-yield point A7 steel. The inelastic plate deformations caused the end

fasteners to continue to pick up load at a faster rate and did not allow as much redistribution as the higher yield point steel did. It can be noted that in the longer A7 steel joint (Fig. 21) the interior bolts contribute very little to the load carrying capacity after the onset of major yielding until an end bolt failed. From one-third to one-half of the innermost bolts were uniformly loaded. The load on the remainder of the bolts increased greatly toward the ends of the joint. This is simply an indication of the relative magnitude of the strain in the main and the lap plates. Near the center of the joint the strains in the main and lap plates were about the same, but near the ends of the joint the strain in one plate became increasingly greater than in the other.

Another factor which influences the load partition in joints is the relative proportions of the bolt shear area and the net tensile area. The influence of this variable is readily apparent in Fig. 18. As a result of the analytical studies reported in Ref. 14, four additional tests of A440 steel joints connected by A325 bolts were performed. Two joints had net tensile areas that were 80% of the bolt shear area and two had net tensile areas equal to 120% of the bolt shear area. It is readily apparent from the test results and theory that with an increase in the net tensile area, the average shear strength of the fasteners for the longer joints is greater. A limiting condition is reached if the net plate area is infinitely greater than the bolt shear area. Under this condition the plate material would be perfectly rigid and each fastener would deform the

same amount and would carry an equal share of the load.

COMPARISON OF HOLE OFFSETS AND JOINT DEFORMATION

Once the theoretical load partition has been accomplished it is possible to determine the predicted hole offsets and compare them with measured values. The predicted hole offsets can be determined as:

$$H = \Delta_i + \eta_i + \eta'_i \tag{18}$$

where H = hole offset,

Δ_i = total deformation of the fastener including the shear, bending, and bearing of the fasteners as well as the bearing deformation of the plate,

η_i = elongation of the radius of the main plate hole, and

η'_i = elongation of the radius of the lap plate hole.

The hole elongations η_i and η'_i were taken from measurements made during the plate calibration tests. Δ_i was computed from Eq. 12. The comparisons are made in Figs. 22 and 23 for four and ten fasteners in a line respectively. There is excellent agreement between the measured hole offsets of the test joints reported in Ref. 17 and the theoretical prediction.

A further comparison between the test results and the theory can be made by comparing the measured load-deformation relationship of the joint with the computed deformations. Such a comparison is made in Fig. 24 for a typical joint. The overall joint deformation between points x-x was computed with the aid of Eqs. 14 and 15. At

any given load the corresponding deformation is given by

$$\text{DEF.} = \text{Slip} + \sum_{i=1}^{n} e_{i,\ i+1} + e_{o1} + e_{nx} \qquad (19)$$

where slip = the measured deformations at each end of the joint between the end bolts and points X. It includes actual joint slip as well as inelastic deformation between the bolts and the points X;

$e_{i,\ i+1}$ = computed main plate elongations within the joint proper; and

e_{o1} and e_{nx} = measured plate elongations between the end bolts and points X.

There is good agreement between the computed deformation given by Eq. 19 and the deformation measured during the test. The agreement held from the time major slip occurred until the joint failed. Thus the theory adequately describes the behavior of bolted joints from slip until ultimate load.

SUMMARY AND CONCLUSIONS

A general theoretical solution for the load partition in double-lap plate splices is developed. This solution is applicable to the region between major joint slip and ultimate load. It is based on the observed behavior of plates with holes and of high-strength bolts in bearing and shear. This solution required the development of analytical expressions for the stress-strain relationship of plates with holes and for the shear-deformation relationship of high-strength bolts. Both expressions are necessarily applicable to both the elastic and inelastic regions. A digital computer program was developed to make the solution practical.

The theoretical solution of load partition and ultimate strength is verified by comparing the theoretical results with the results of tests of eight large A7 steel bolted joints and eleven large A440 steel bolted joints. In all cases the theory and tests results are in good agreement. The greatest difference between the theoretical and experimental results is approximately 4%.

It is shown that the decrease in average ultimate shear strength as the length of joint is increased is greater for "balanced" A7 steel joints than for "balanced" A440 steel joints connected with A325 bolts. A study of varying the relative proportions of the bolt shear area and the net tensile area shows that an increase in the net plate area increases the average shear strength of the fasteners in the longer joints.

Experimental studies verify this behavior. Also, the balanced design concept is shown to have little meaning. A joint can only be in balance for a specific length and specific ratio of bolt shear area to net tensile area of the plate.

ACKNOWLEDGEMENTS

The study described in this paper is part of an investigation of large bolted joints being conducted at Fritz Engineering Laboratory, Department of Civil Engineering, Lehigh University. Professor W. J. Eney is head of the Department and Laboratory and Dr. L. S. Beedle is director of the Laboratory. The project is financed by the Pennsylvania Department of Highways, the Department of Commerce - Bureau of Public Roads, the American Institute of Steel Construction, and the Research Council on Riveted and Bolted Structural Joints.

The authors are particularly indebted to Dr. L. S. Beedle for his supervision and encouragement while serving as Project director and also as Professor in charge of the dissertations on which this report is based. Sincere thanks are also due the guiding Committee of the Research Council on Riveted and Bolted Structural Joints.

TABLE 1

SUMMARY OF TEST RESULTS AND ANALYSIS OF A325 BOLTS

Bolt Lot	Type Conn. Matl.	Type Test Jig	Ult. Strength R_{ult}, kips	Bolt Parameters μ	λ	Ult. Deform. Δ_{ult}, in.
8A	A440	Tension	98.6	23	1	0.187
8A	A440	Compression	102.3	23	1	0.200
8B	A440	Tension	92.5	25	0.95	0.200
8B	A440	Compression	104.0	22	1	0.239
H	A440	Tension	95.2	22	1	0.220
H	A440	Compression	103.0	22	1	0.236
C	A7	Tension	98.5	18	1	0.238
C	A7	Compression	106.9	18	1	0.291
D	A7	Tension	101.8	18	1	0.279
D	A7	Compression	102.5	18	1	0.300

TABLE 2

COMPARISON OF THEORETICAL AND EXPERIMENTAL ULTIMATE LOADS
A7 STEEL JOINTS

Joint	$\frac{A_n}{A_s}$	Load at Failure kips	COMPUTED ULTIMATE STRENGTH, KIPS Method 1	$\frac{\text{Computed}}{\text{Observed}}$	Method 2	Method 3	$\frac{\text{Computed}}{\text{Observed}}$
D71	1.10	1126	1123	0.997	1118	1142	1.014
D81	1.10	1282	1232	0.961	1232	1252	0.977
D91	1.10	1358	1365	1.005	1370	1389	1.023
D101	1.10	1506	1445	0.959	1451	1470	0.976
D10	1.10	1544	1434	0.929	1441	1550	1.004
D13A	1.10	1988	1823	0.917	1839	1969	0.990
D13	1.10	1954	1724	0.930	1736	1858	1.002
D16	1.10	2085	1997	0.958	2014	2146	1.029

TABLE 3

COMPARISON OF THEORETICAL AND EXPERIMENTAL ULTIMATE LOADS
A440 STEEL JOINTS

Joint	$\frac{A_n}{A_s}$	Load at Failure kips	COMPUTED ULTIMATE STRENGTH, KIPS Method 1	$\frac{\text{Computed}}{\text{Observed}}$	Method 2	Method 3	$\frac{\text{Computed}}{\text{Observed}}$
E41	1.00	728	730	1.003	699	800	1.099
E41F	1.00	727	730	1.003	699	800	1.099
E41G	1.00	767	767	1.000	757	798	1.040
E71	1.00	1188	1209	1.018	1193	1320	1.111
E101	1.00	1610	1604	0.996	1596	1720	1.068
E131	1.00	2125	2062	0.970	2074	2155	1.014
E161	1.00	2545	2425	0.953	2446	2526	0.993
E721	0.80	1070	1086	1.015	1075	1147	1.071
E163	0.80	2180	2080	.954	2094	2164	.993
E722	1.20	1270	1268	.998	1224	1392	1.096
E164	1.20	2785	2720	.977	2726	2842	1.020

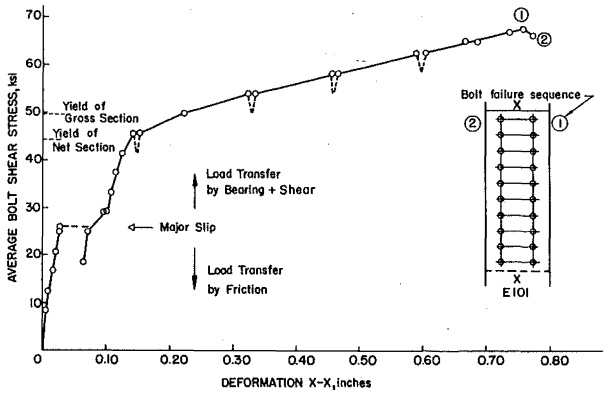

Fig. 1 Typical Load-Deformation Curve

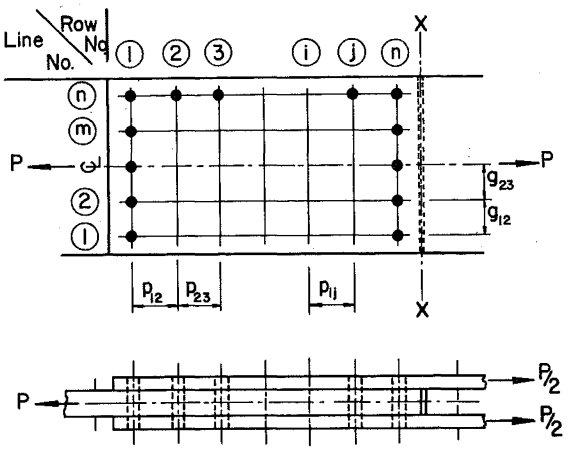

Fig. 2 Joint Geometry

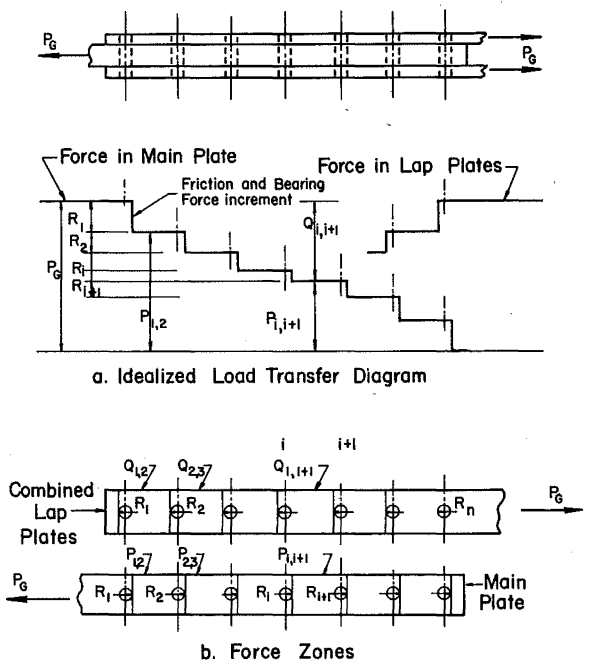

Fig. 4 Idealized Load Transfer

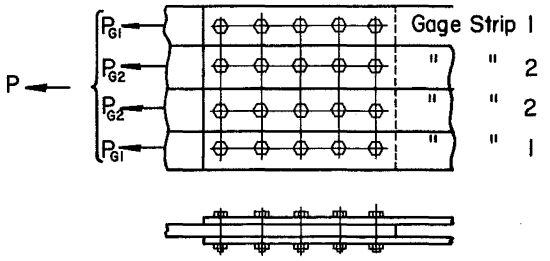

Fig. 3 Division of Joint into Gage Strips

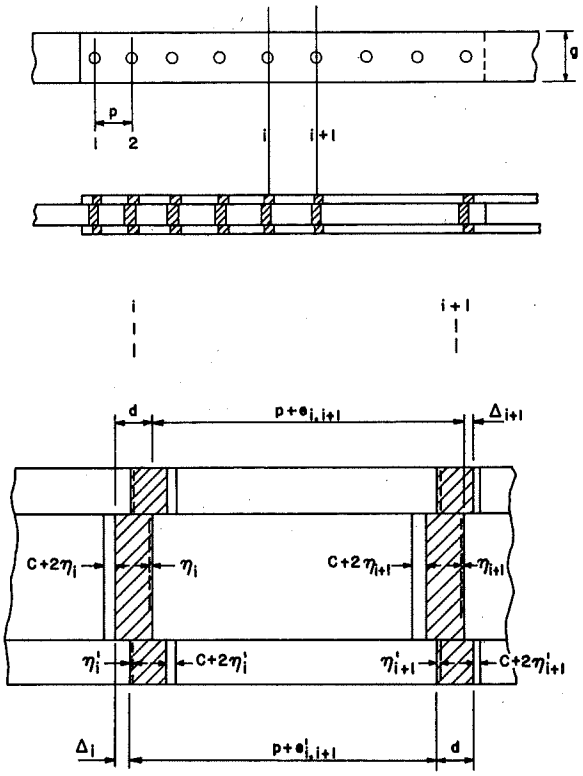

Fig. 5 Deformations in Bolts and Plates

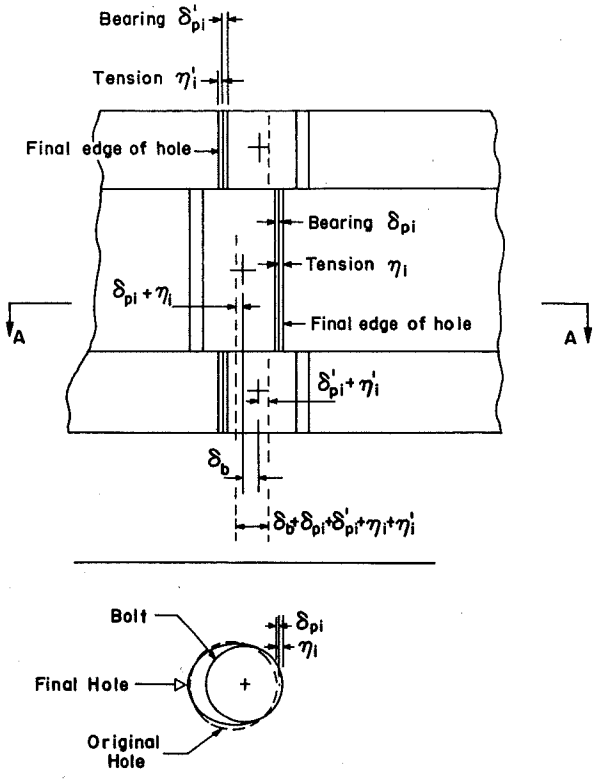

Fig. 6 Relation of Hole and Bolt Deformations

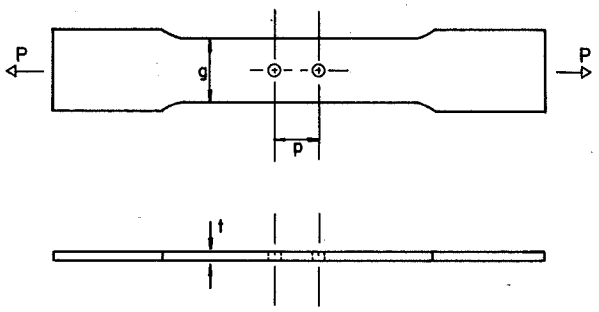

Fig. 7 Schematic of Plate Calibration Coupon

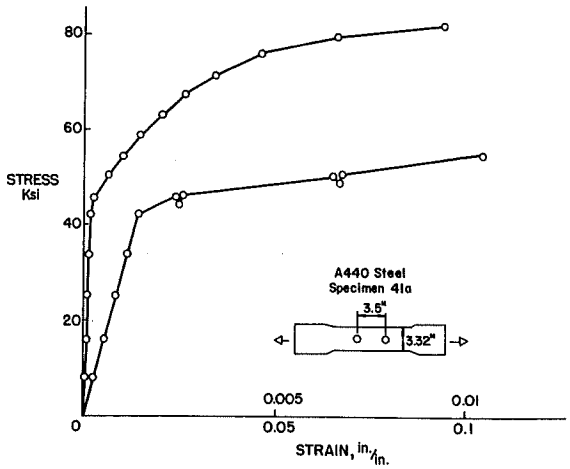

Fig. 8 Typical Stress-Strain Diagram for Plate Calibration Coupon

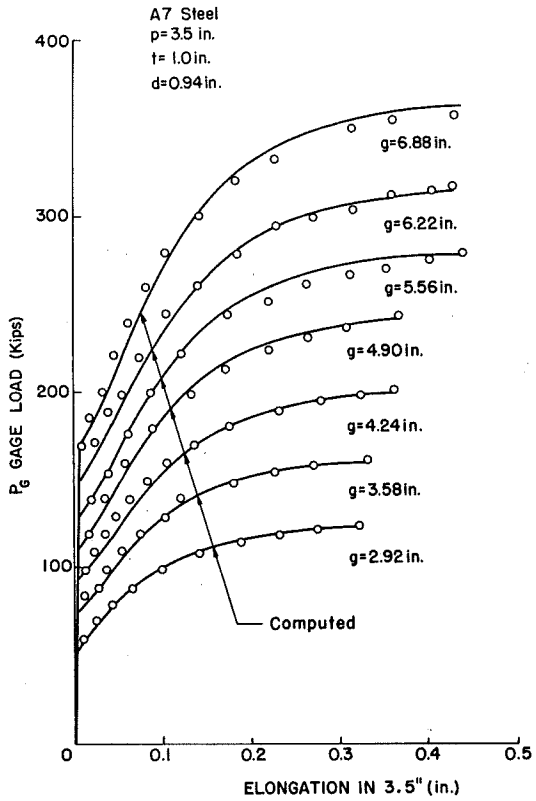

Fig. 9 Summary of Plate Calibration Tests for A7 Steel Plate

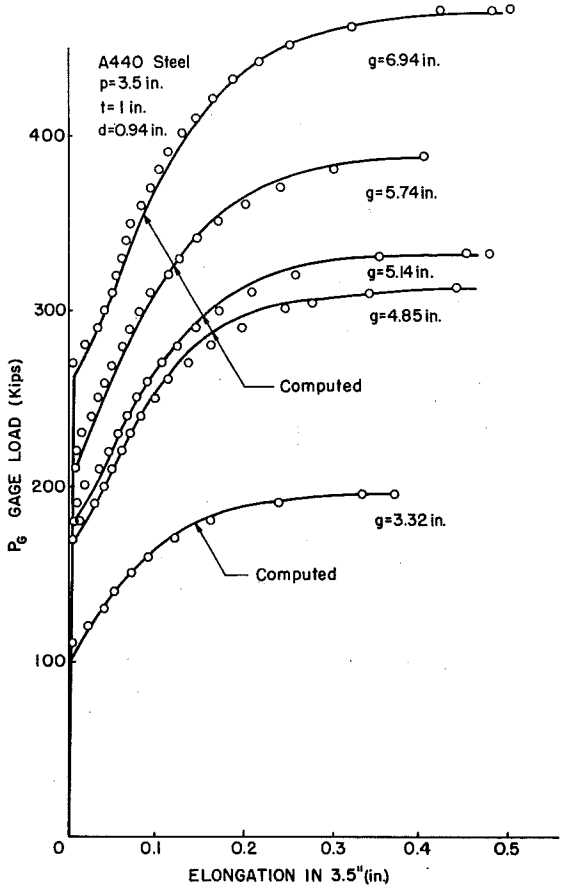

Fig. 10 Summary of Plate Calibration Tests for A440 Steel Plate

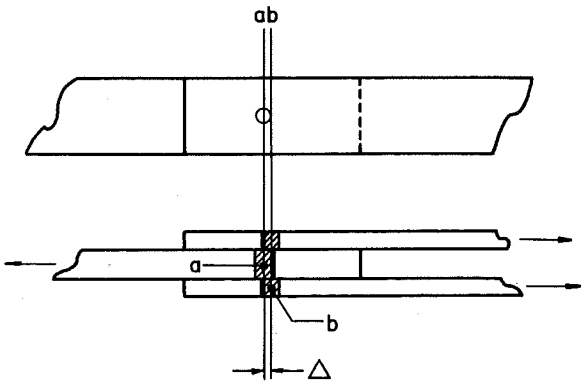

Fig. 11 Deformation of a Single Bolt

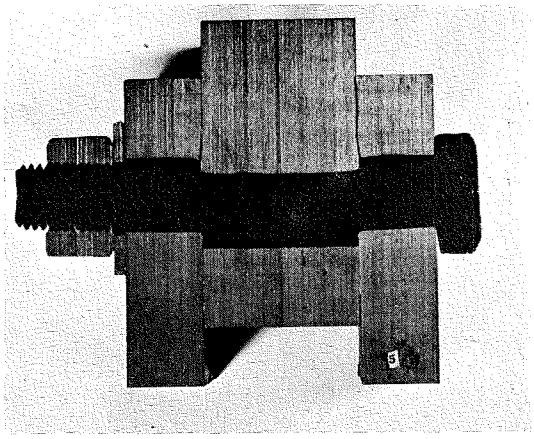

Fig. 12 Sawed Section of a Single Bolt

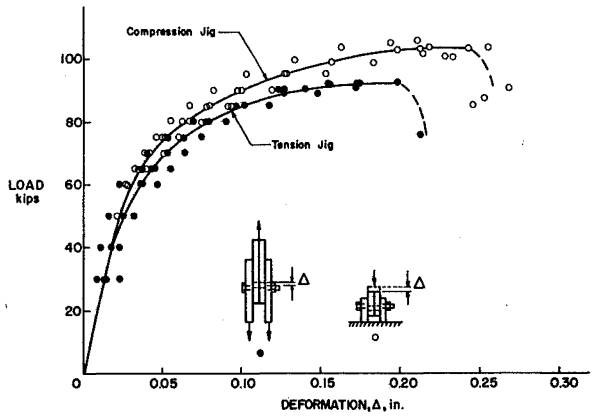

Fig. 13 Typical Load-Deformation Curves for A325 Bolts Connecting A440 Steel

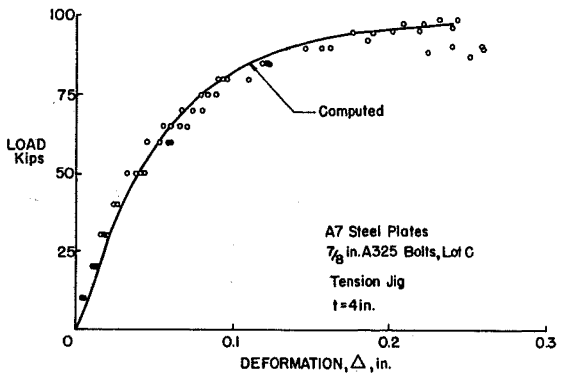

Fig. 14 Typical Load-Deformation Relationship for A325 Bolts in A7 Steel

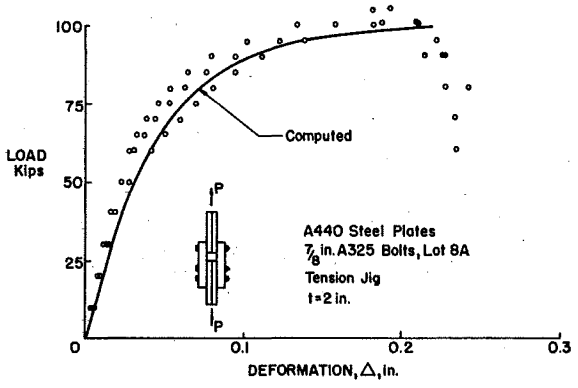

Fig. 15 Typical Load-Deformation Relationship for A325 Bolts in A440 Steel

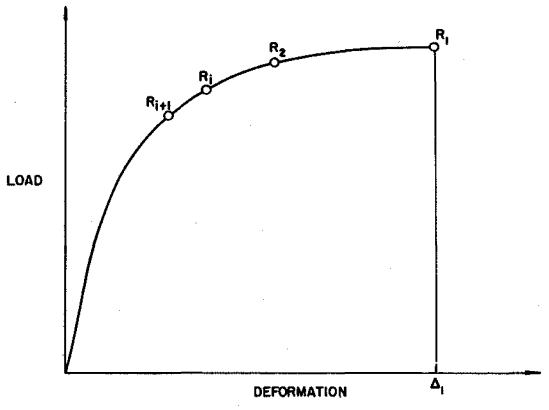

Fig. 16 Location of Bolt Forces on Load-Deformation Curve

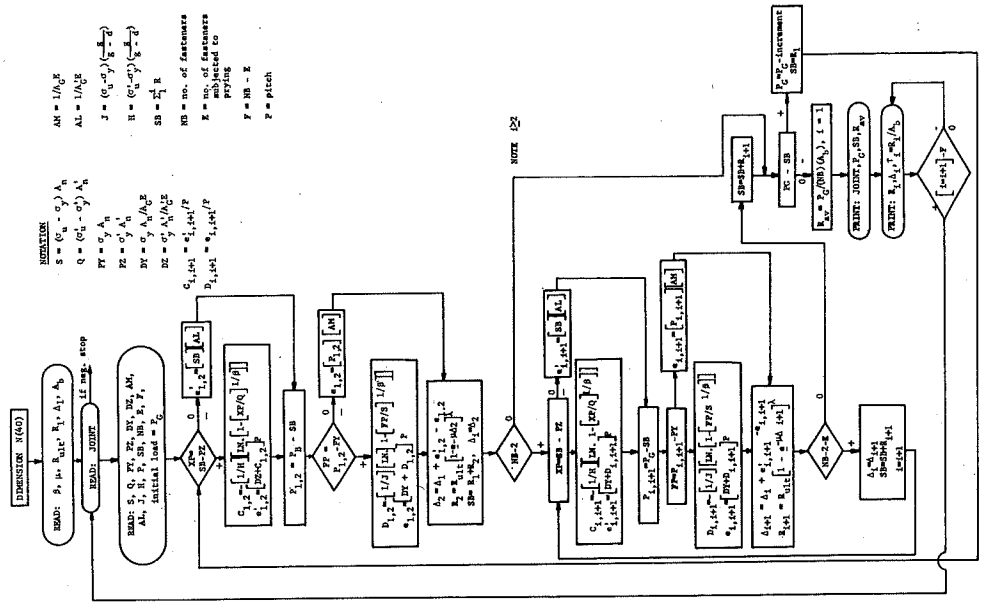

Fig. 17 Flow Diagram for Load Partition Computations

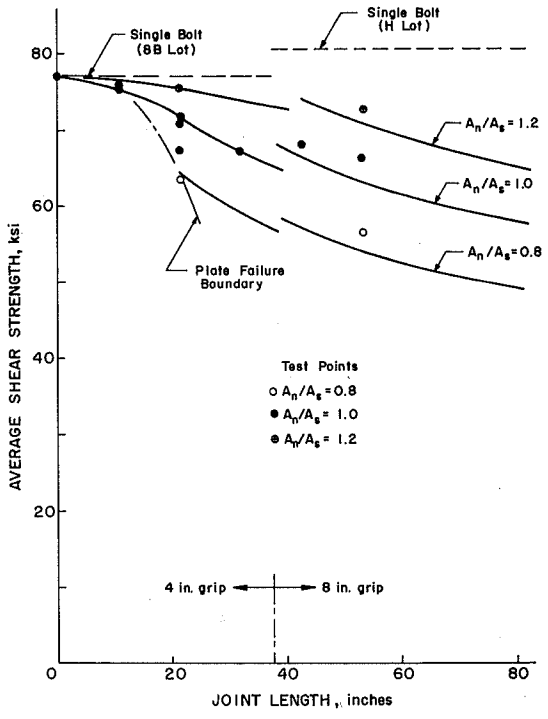

Fig. 18 Comparison of Computed Ultimate Strength with Test Results of A440 Steel Joints

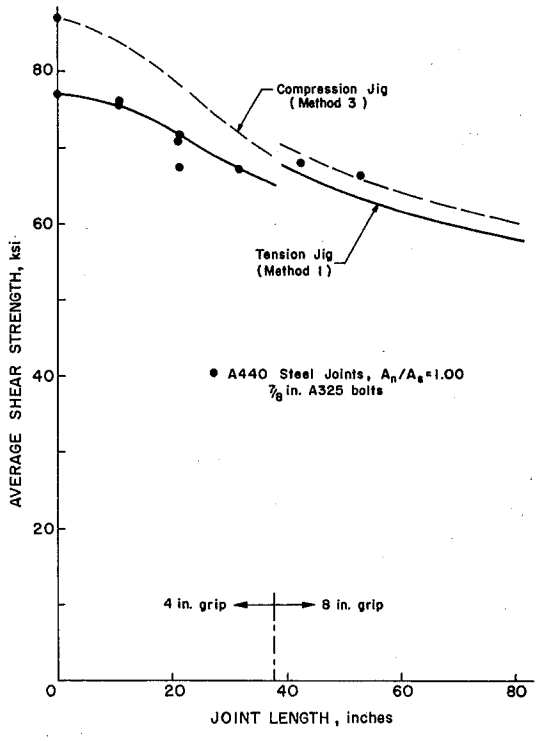

Fig. 19 Comparison of Methods 1 and 3 with Experimental Results

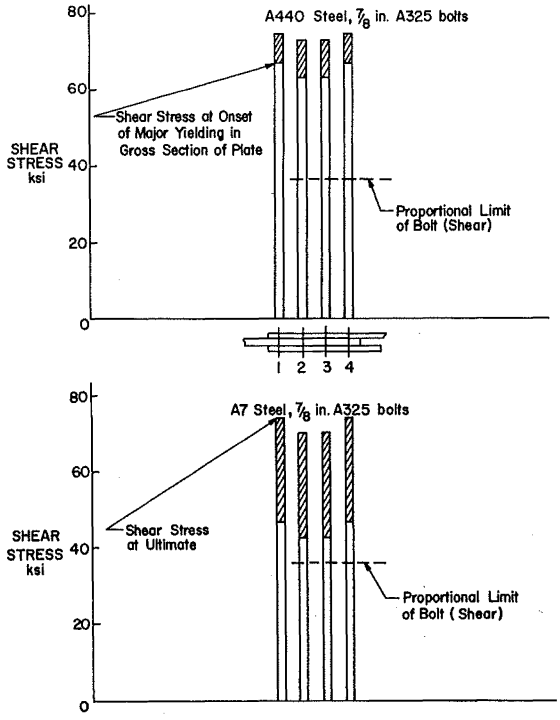

Fig. 20 Load Partition in Joints with Four Fasteners in Line

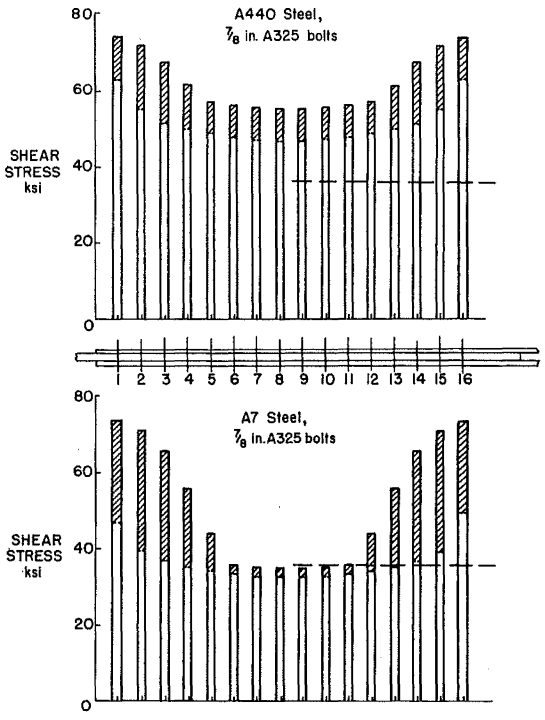

Fig. 21 Load Partition in Joints with Sixteen Fasteners in Line

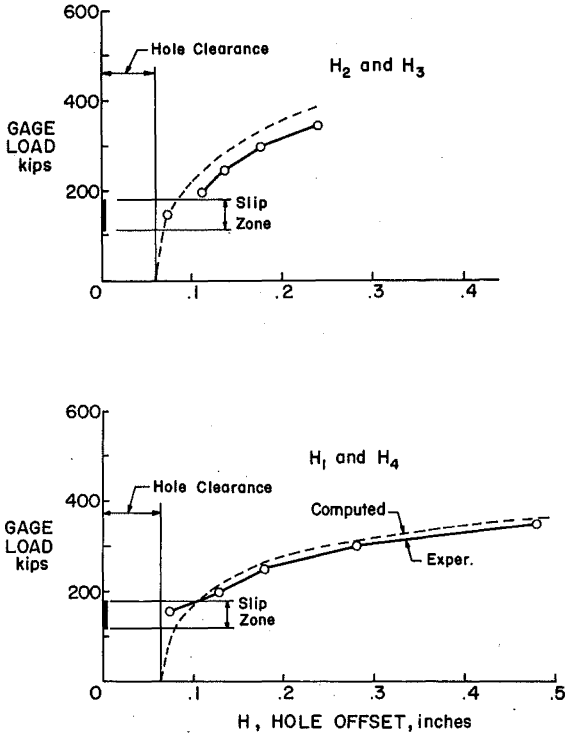

Fig. 22 Comparison of Computed and Experimental Hole Offsets - Joint D41

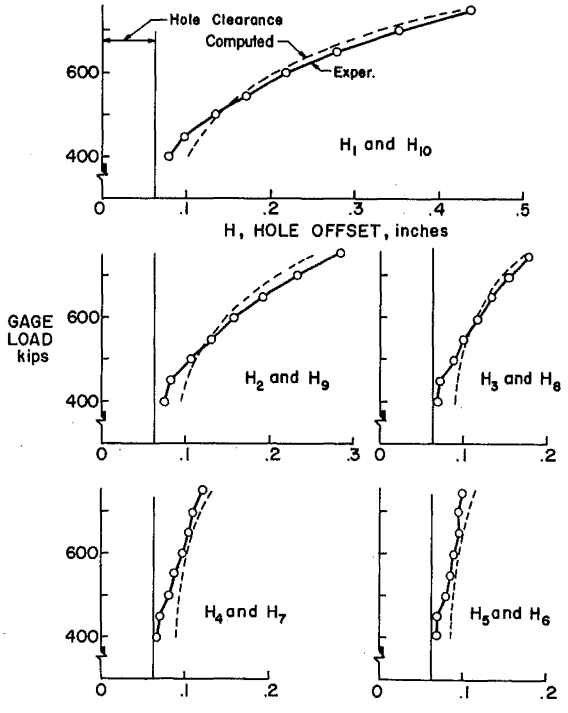

Fig. 23 Comparison of Computed and Experimental Hole Offsets - Joint D101

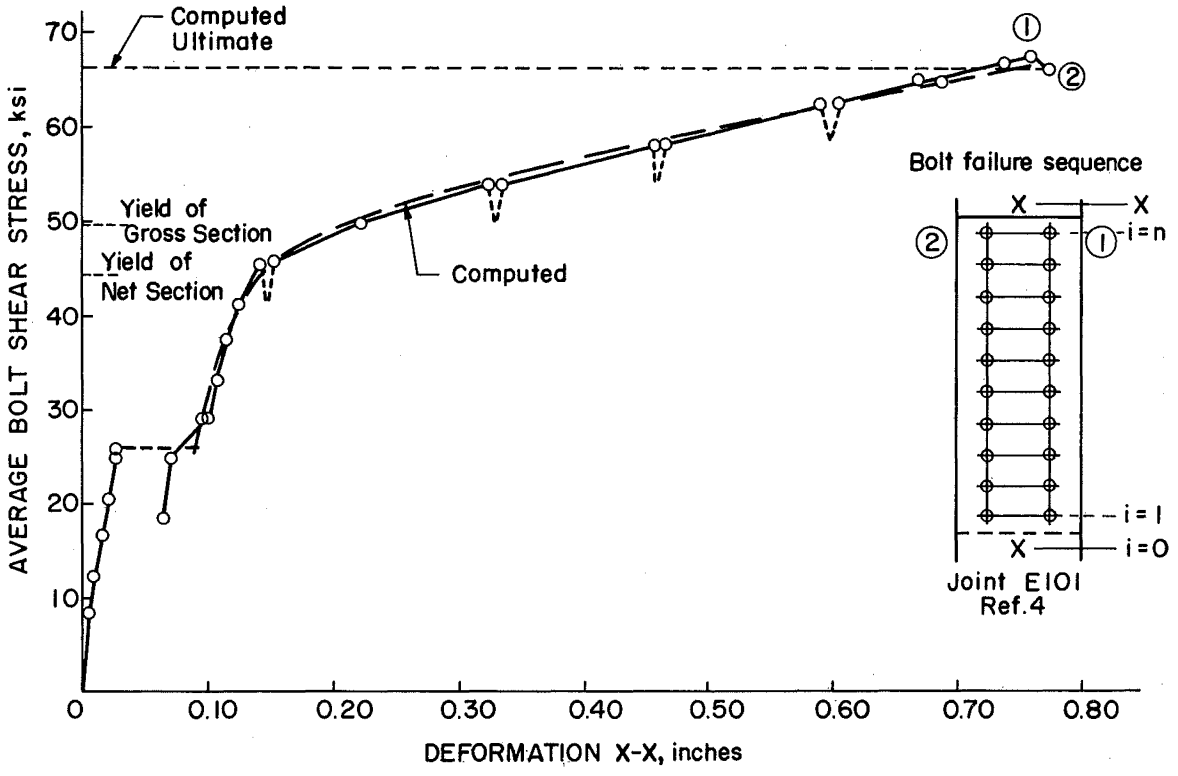

Fig. 24 Comparison of Computed and Experimental Joint Deformation

REFERENCES

1. Davis, R. E., Woodruff, G. B., and Davis, H. E.
   TENSION TESTS OF LARGE RIVETED JOINTS
   Transactions ASCE, Vol. 105, p. 1193, (1940)

2. SPECIFICATIONS FOR ASSEMBLY OF STRUCTURAL JOINTS
   USING HIGH STRENGTH BOLTS
   (1951), Research Council on Riveted and Bolted
   Structural Joints of the Engineering Foundation

3. Foreman, R. T., and Rumpf, J. L.
   STATIC TENSION TESTS OF COMPACT BOLTED JOINTS
   Transactions ASCE, Vol. 126, Part II, p. 228, (1961)

4. Fisher, J. W., Ramseier, P. O., and Beedle, L. S.
   TESTS OF A440 STEEL JOINTS FASTENED WITH A325 BOLTS
   Publications IABSE, Vol. 23, (1963)

5. Fisher, J. W., and Beedle, L. S.
   CRITERIA FOR DESIGNING BOLTED JOINTS (BEARING-TYPE)
   Fritz Laboratory Report 288.7A, Lehigh University,
   Bethlehem, Pa., (1964)

6. De Jonge, A. E. R.
   RIVETED JOINTS: A CRITICAL REVIEW OF THE LITERATURE
   COVERING THEIR DEVELOPMENT
   ASME, New York, (1945)

7. Hrennikoff, A.
   THE WORK OF RIVETS IN RIVETED JOINTS
   Transactions, ASCE, Vol. 99, pp. 437-489, (1939)

8. Arnovlevic, I.
   INANSPRUNCHNAHME DER ANSCHLUSSNIETEN ELASTISCHER STABE
   Seitschrift fur Architekten und Ingenieure, Vol. 14,
   Heft, 2, p. 89, (1909)

9. Batho, C.
   THE PARTITION OF LOAD IN RIVETED JOINTS
   Journal of the Franklin Institute, Vol. 182, p. 553,
   (1916)

10. Bleich, F.
    THEORIE UND BERECHNUNG DER EISERNER BRUCKER
    Julius Springer, Berlin, (1931)

11. Vogt, F.
LOAD DISTRIBUTION IN BOLTED OR RIVETED STRUCTURAL JOINTS IN LIGHT-ALLOY STRUCTURES
U. S. NACA Tech. Memo No. 1135, (1947)

12. Francis, A. J.
THE BEHAVIOR OF ALUMINUM ALLOY RIVETED JOINTS
The Aluminium Development Association, Research Report No. 15, London, (1953)

13. Rumpf, J. L.
THE ULTIMATE STRENGTH OF BOLTED CONNECTIONS
Ph.D. Dissertation, Lehigh University, Bethlehem, Pa., (1960)

14. Fisher, J. W.
THE ANALYSIS OF BOLTED PLACE SPLICES
Ph.D. Dissertation, Lehigh University, Bethlehem, Pa., (1964)

15. Wyly, L. T., Treaner, H. E., and LeRoy, H. E.
DEMONSTRATION TEST OF A242 HIGH STRENGTH STEEL SPECIMEN CONNECTED BY A325 AND A354 BD BOLTS
AISC Proceedings, (1957)

16. Vasarhelyi, D. D., Benno, S. Y., Madison, R. B., Lu, Z. A., and Vasishth, U. C.
EFFECTS OF FABRICATION TECHNIQUES
Transactions ASCE, Vol. 126, Part II, (1961)

17. Bendigo, R. A., Hansen, R. M., and Rumpf, J. L.
LONG BOLTED JOINTS
Journal of the Structural Division, ASCE, Vol. 89, ST6, (1963)

18. Steinhardt, O., and Mohler, K.
VERSUCHE ZUR ANWENDUNG VORGESPANNTER SCHRAUBWN IM STAHLBAU
II Teil, Stahlbau-Verlags-Gmblt, Cologne, (1959)

19. Wallaert, J. J., and Fisher, J. W.
HISTORY OF INTERNAL TENSION IN BOLTS CONNECTING LARGE JOINTS
Fritz Engineering Laboratory Report 288.13, Lehigh University, Bethlehem, Pa., (in preparation)

20. Coker, E. G.
THE DISTRIBUTION OF STRESS DUE TO A RIVET IN A PLATE
Transactions, Institute of Naval Arch., Vol. 55, p. 207, (1913)